Supplementary Information

Remarkable Photostability Enhancement in $FAPbBr_3$ Perovskite Nanocrystal Polymer Films via Lecithin Passivation

Takuro Iizuka[a], Naoaki Oshita[a], Shunya Abe[a], Khang Vinh Huynh[b], Rinku Watanabe[b], Yuta Ito[a], Takao Oto[a], Satoshi Asakura[c], Motofumi Kashiwagi[d], and Akito Masuhara[a,e]*

a. Graduate School of Science and Engineering, Yamagata University, 4-3-16, Jonan, Yonezawa, Yamagata 992-8510, Japan

b. Faculty of Engineering, Yamagata University, 4-3-16 Jonan, Yonezawa, Yamagata, 992-8510, Japan

c. ISE CHEMICALS Corporation, 1-3-1 Kyobashi, Chuo-ku, Tokyo, 104-0031, Japan.

d. ZEON Corporation, 1-6-2 Marunouchi, Chiyoda-ku, Tokyo, 100-8246, Japan.

e. Frontier Center for Organic Materials (FROM), Yamagata University, 4-3-16 Jonan, Yonezawa, Yamagata, 992-8510, Japan

*Corresponding author: masuhara@yz.yamagata-u.ac.jp

Experimental method

Materials

N, N-dimethylformamide (DMF, 99.5%), dimethyl carbonate (DMC, 98.0%), propylene glycol 1-monomethyl ether 2-acetate (PEG-MEA, >98%), tri-*n*-octylphosphine oxide (TOPO, >95.0%), didodecyldimethylammonium bromide (DDAB, >98.0%), cesium carbonate (Cs_2CO_3, >98.0%), potassium bromide (KBr, >99.0%), lead bromide ($PbBr_2$, 98%), lead iodide (PbI_2, 99.99%), formamidine hydrobromide (FABr, 99.99%) were purchased from Tokyo Chemical Industry Co., Ltd. Toluene (>99.5%), lecithin (1st.

grade), were purchased from Wako Pure Chemical Co., Osaka, Japan. Oleic acid (OA, >90%), octylamine (OcAm, 99%) was purchased from Sigma-Aldrich Japan Co., Tokyo, Japan respectively. Cyclic olefin polymer (COP) was provided by Zeon Co., Tokyo, Japan. All reagents were used without any purification.

Preparation of Control and Target $FAPbBr_3$ PeNC dispersions

220 mg of $PbBr_2$, 75 mg of FABr were dissolved in 1 mL of DMF to prepare a precursor solution. The precursor solution (900 μL) was injected into the poor solvent, which consisted of 630 μL of OA, 39 μL of OcAm dissolved in 15 mL of PEG-MEA under vigorous stirring. The solution immediately turned a turbid yellowish-green color and was mixed for 3 min. After that, 7.5 mL of DMC was added to the mixture. The crude PeNCs were collected and centrifuged at 16,500 rpm for 3 min, and the supernatant was removed. The precipitate was added to 12 mL of toluene and redispersed in the solvent. The dispersions were centrifuged again at 16,500 rpm for 2 min to collect the PeNC dispersion as the **Control**. And then 240 μL of the ligand solution, in which 0.5 mmol of lecithin dissolved in 1 mL toluene, was added to the PeNC dispersion as the **Target**.

Preparation of red-emission $CsPbBr_{1-x}I_x$ PeNC dispersions [1]

・Preparation of Precursor and Ligand Solutions

All solutions were stirred overnight after preparation and then used.

・Precursor Solution ①: 275.3 mg $PbBr_2$ and 1159.8 mg of TOPO were dissolved in 15 mL of toluene.

・**Precursor Solution** ②**:** 691.5 mg of PbI_2 and 2319.6 mg of TOPO were dissolved in 30 mL of toluene.
・**Precursor Solution** ③**:** 11.9 mg of KBr and 5680 μL of OA were dissolved in 10 mL of toluene.
・**Precursor Solution** ④**:** 977.4 mg of Cs_2CO_3 and 5680 μL of OA were dissolved in 10 mL of toluene.

・**Ligand Solution:** 185.1 mg of DDAB was dissolved in 3 mL of toluene.

The procedures of red-emission PeNC precursor solutions

1500 μL of Precursor Solution ①, 5050 μL of Precursor Solution ②, and 525 μL of Precursor Solution ③ were mixed. Subsequently, 500 μL of Precursor Solution ④ was added to the mixture to promote the crystal growth of PeNCs, followed by stirring for 5 min. To terminate the crystal growth process, 56 μL of the Ligand Solution was added, and the resulting mixture was stirred for an additional 2 min. The purification process was conducted as follows: 5500 μL of DMC was added to the solution, and the mixture was centrifuged at 16,500 rpm for 3 min. After discarding the supernatant, the precipitate was redispersed in 5000 μL of toluene. Finally, the dispersion was centrifuged again at 16,500 rpm for 2 min, and the purified PeNC dispersion was collected.

Preparation of PeNC polymer films

A polymer solution was prepared by dissolving the polymer matrix in toluene at a concentration of 40 wt%. To prepare the PeNC–polymer solution, 7 g of the polymer solution was mixed with 1500 μL of the as-synthesized PeNC dispersion. The mixture was processed using a planetary centrifugal mixer at 2000 rpm for 5 min, followed by vacuum degassing at 2200 rpm for 30 s. The resulting PeNC polymer solution was

then cast by the doctor-blade method. Finally, the composite films were dried at room temperature for 30 min to complete the film formation process.

Fabrication of the on-chip White LED (WLED)

WLEDs were fabricated by stacking green- and red-emitting PeNC polymer films onto a commercially available blue inorganic LED chip. The PeNC polymer films were stacked such that the red-emitting PeNC polymer film was placed directly on the blue LED, followed by the green-emitting PeNC polymer film. Bright white light emission was obtained by combining the transmitted blue light with the PL emitted from the green- and red-emitting PeNC polymer films. For spectral measurements, the blue LED was operated at a constant current of 1 mA. No encapsulation was applied to the devices. All measurements were carried out under ambient conditions at room temperature.

Quantitative ^{1}H NMR

The PeNC dispersion was washed once by DMC to remove free ligands for ^{1}H NMR measurements of the ligands. The solvent in the PeNC dispersion was then completely removed using an evaporator. The dried PeNCs were added to 650 μL of DMSO-d_6, and 50 μL of 0.2 mmol/mL of maleic acid solution in DMSO-d_6 was added. Maleic acid was used as the reference material. DMSO-d_6 was used to decompose the PeNC crystal structure to avoid the negative effects of the PeNC crystals on the spectrum. The molar concentrations of the ligands were calculated as follows. It is shown in Fig. S3, Table S5, and Table S6 were calculated using the method reported by Kimura *et al*., following the procedure described below. In ^{1}H NMR, the integral intensity is

proportional to the number of protons.[2] The signal intensity in ^{1}H NMR for two substances (each ligand and maleic acid as a reference substance) can be expressed by the following equation (1)

$$C_{Ligand} = \frac{I_{Maleic\ Acid}}{I_{Ligand}} \times \frac{H_{Maleic\ Acid}}{H_{Ligand}} \times C_{Maleic\ acid} \quad (1)$$

where *I* is the signal intensity (integrated value), *H* is the number of protons in the functional group, and *C* is the concentration of the substance.

1. The intensity(integrated) ratio of the peaks derived from maleic acid, which was added to the NMR sample in a known amount, and the peaks derived from the OA, OcAm, and lecithin were calculated by considering the number of protons.
2. The molar amount of each ligand was determined based on the peak intensity ratio and the molar amount of maleic acid.
3. The molar concentration was obtained by dividing the molar amount by the volume of the added PeNC dispersion sample.

Characterization

The crystal morphology and structure of the PeNC were characterized by transmission electron microscope (TEM, JEOL JEM-2100F) operated at an accelerating voltage of 200 kV. The hydrodynamic size distribution of the PeNCs was evaluated by dynamic light scattering (DLS, Microtrac Nanotrac FLEX), using dispersions prepared in toluene at the appropriate concentration of the device. X-ray diffraction (XRD) patterns were recorded using a Rigaku SmartLab diffractometer equipped with Cu Kα radiation (λ =

1.54 Å), operated at 45 kV and 100 mA. Fourier transform infrared (FT-IR) spectra were measured using a Jasco FT/IR-4000 spectrometer with an ATR PRO ONE X accessory. X-ray photoelectron spectroscopy (XPS) measurements were carried out using a Thermo Fisher Scientific Nexsa G2 spectrometer with Al Kα radiation. The binding energies were calibrated to the C 1s peak at 284.8 eV. Photoluminescence (PL) spectra and photoluminescence quantum yield (PLQY) were measured using a Jasco FP-8600 spectrometer equipped with an integrating sphere using a JASCO ILF-835 100 mm φ. Absolute PLQY values were obtained under excitation at 370 nm for PeNC dispersions and 450 nm for PeNC polymer films. All PL measurements were conducted at room temperature. Time-resolved photoluminescence (TRPL) measurements were performed using a Hamamatsu C11367 Quantaurus-Tau system. The PL decay curves were fitted using a biexponential function after reconvolution with the instrument response function (IRF). The average PL lifetime (τ_{avg}), radiative recombination rate constant (K_r), and nonradiative recombination rate constant (K_{nr}) were calculated using the following equations (2)–(6), assuming a biexponential decay model:

$$\tau_{avg.} = \frac{\sum_{i=1}^{n} A_i \tau_i^2}{\sum_{i=1}^{n} A_i \tau_i} \quad (2)$$

$$\frac{1}{\tau_{avg.}} = k_{rad} + k_{nonrad} \quad (3)$$

$$\mathrm{PLQY} = \frac{k_{rad}}{k_{rad} + k_{nonrad}} \quad (4)$$

$$K_{rad} = \frac{PLQY}{\tau_{avg.}} \quad (5)$$

$$K_{nonrad} = \frac{1 - PLQY}{\tau_{avg.}} \quad (6)$$

Ultraviolet–visible (UV–vis) absorption spectra were recorded using a Jasco V-670 spectrometer in the wavelength range of 300–700 nm.

Scanning electron microscopy–energy dispersive X-ray spectroscope (SEM-EDX) measurements were performed using a JEOL JSM-IT800 microscope operated at an accelerating voltage of 10 kV. The samples for SEM-EDX analysis were prepared by drop casting. The transient absorption (TA) spectra were obtained using a conventional pump-probe setup (Helios, Ultrafast Systems). The pump light pulses at 450 nm were delivered from an optical parametric amplifier (TOPAS, Light Conversion) driven by an amplified Ti:Sapphire laser system (Spitfire, Spectra-Physics). A fraction of the fundamental output (800 nm, 80 fs, 1 kHz) was converted to white light for the probe pulses. The delay time between the pump and probe pulse was controlled by an optical delay line. For a quantitative discussion of the obtained TA spectra, the data were analyzed using a biexponential fitting function, where the average lifetime ($\tau_{avg.}$) was determined according to Equation (2). Electroluminescence (EL) spectra were recorded using an Ocean Insight FLAME-S-UV-VIS spectrometer. The devices were operated under constant-current driving at 1 mA. All measurements were carried out at room temperature under ambient conditions without encapsulation.

2. Supporting results

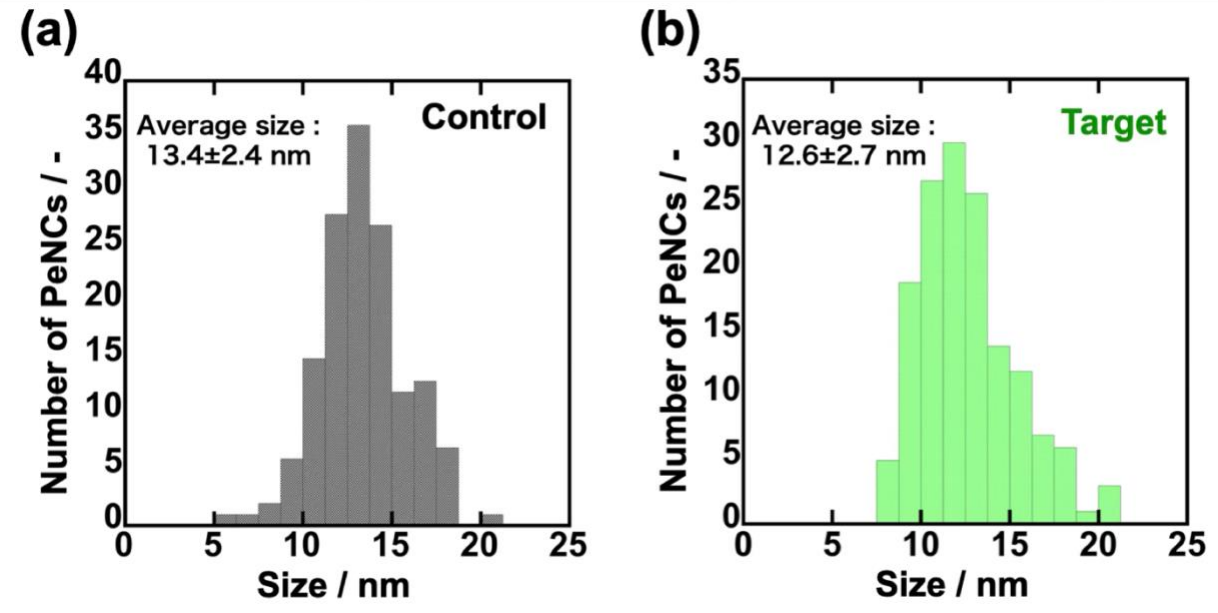

Fig. S1(a)-(b) Size distribution of PeNCs from TEM images

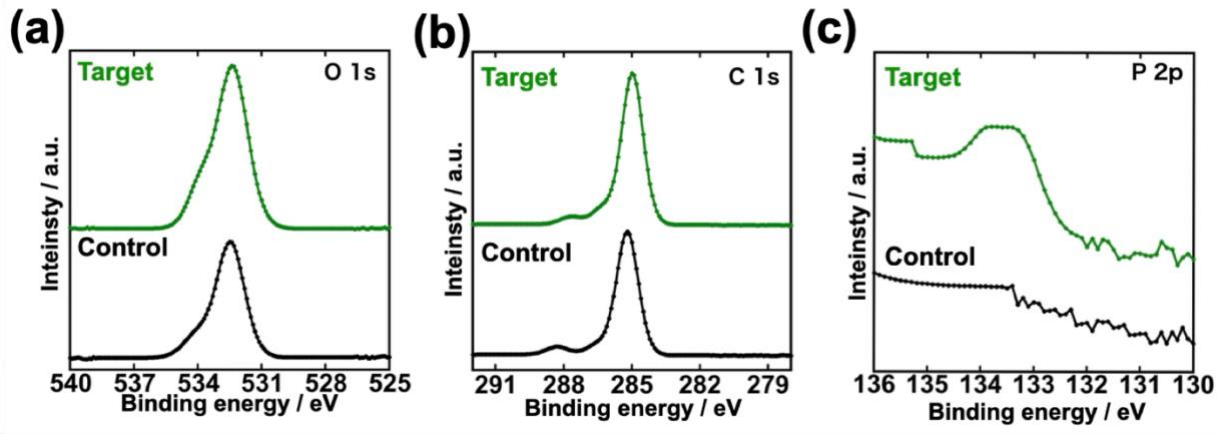

Fig. S2 XPS spectra of each PeNC. (a) O 1s, (b) C 1s, (c) P 2p

Table S1 Atomic ratio on the PeNC surface by XPS

Sample	Atomic ratio / %		
	Pb	Br	P
Control	1	3.85	-
Target	1	3.63	0.13

Table S2 The binding energy of Pb 4f

Sample	Pb 4f	
	4f 5/2 /eV	4f 7/2 /eV
Control	143.2	138.3
Target	143.1	138.2

Table S3 The binding energy of Br 3d

Sample	Br 3d	
	3d 3/2 /eV	3d 5/2 /eV
Control	68.2	69.3
Target	68.1	69.2

Table S4 The binding energy of N 1s

Sample	N 1s	
	NH_2 /eV	NH_3^+ /eV
Control	401.9	400.0
Target	401.8	400.1

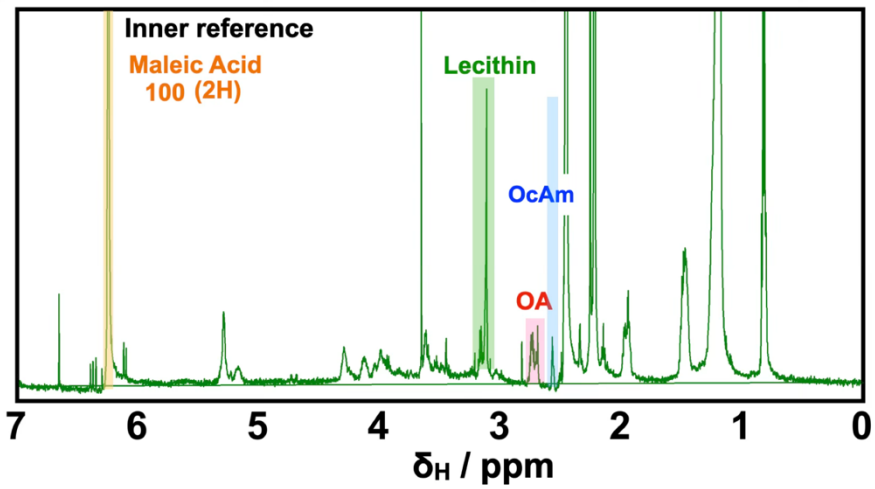

Fig. S3 Quantitative ^{1}H NMR evaluation of ligands in purified in PeNCs dispersion

Table S5 Ligand concentration obtained from quantitative ^{1}H NMR

Sample	Ligand concentration / μmol/ mL				
	Inner reference	OA	OcAm	Lecithin	Total ligands
Target	7.80	0.63	0.22	0.29	1.14

Table S6 Calculation result of ligand proportion in the purified PeNC dispersion

Sample	Ligand proportion / %			
	OA	OcAm	Lecithin	Total ligands
Target	55.0	19.3	25.8	100

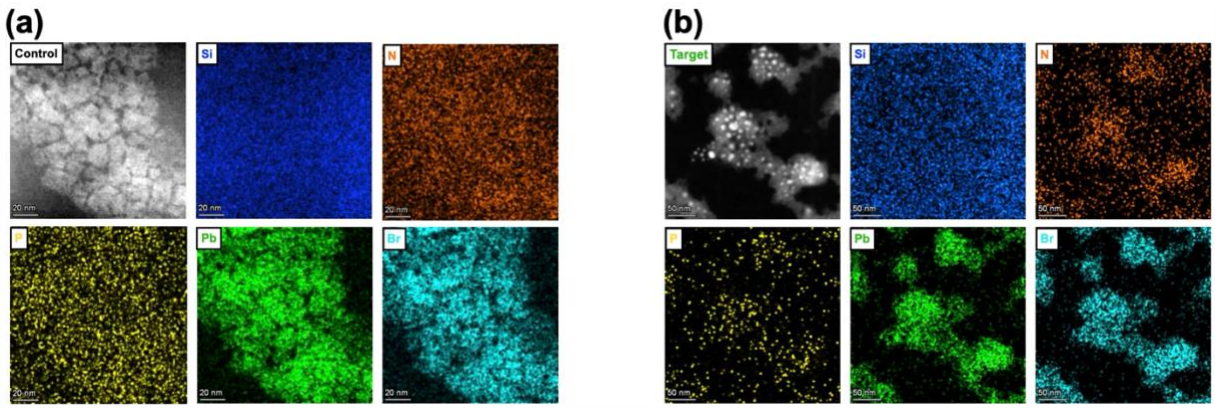

Fig. S4 STEM HAADF and EDX mapping images of (a) Control and (b) Target samples. Individual maps represent Si (blue), N (orange), P (yellow), Pb (green), and Br (cyan).

Note: TEM-EDX images reflect electron beam damage; size and morphology are evaluated from TEM images (Fig. 1(b)–(c), Fig. S1(a)–(b)).

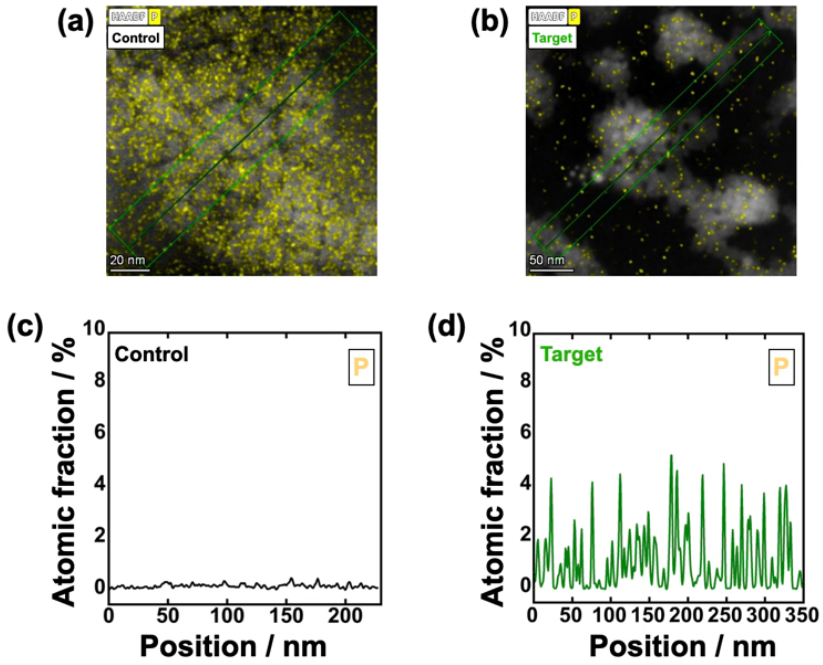

Fig. S5 HAADF-STEM and EDX analysis of Control and Target samples. (a, b) Overlay of HAADF-STEM images and P elemental maps. Green boxes indicate the areas selected for line profiles (c, d) . Phosphorus atomic corresponding to the areas highlighted in (a) and (b) respectively.

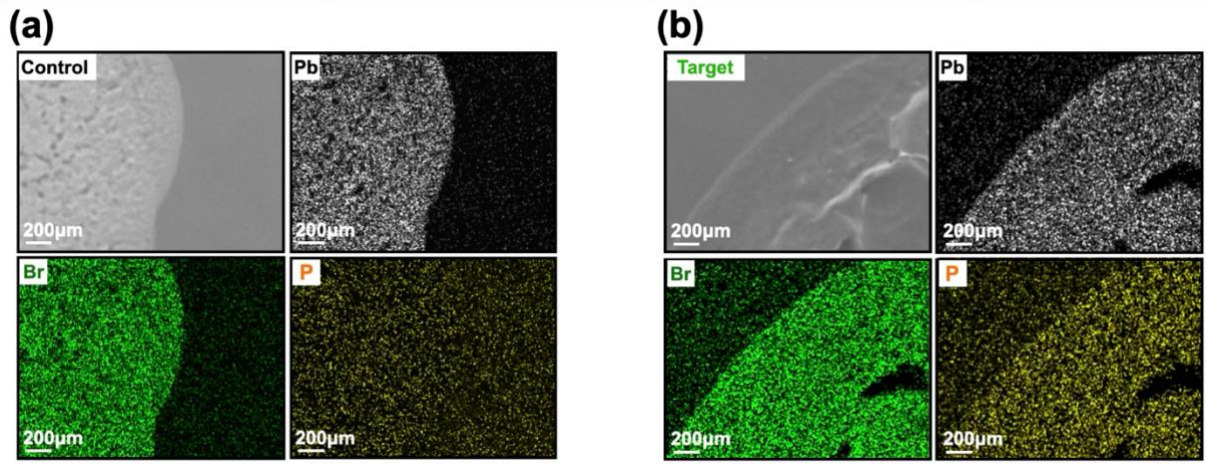

Fig. S6 SEM images and corresponding EDX elemental maps of (a) Control and (b) Target samples. The maps show the distribution of Pb (white), Br (green), and P (yellow). Scale bars: 200 μm.

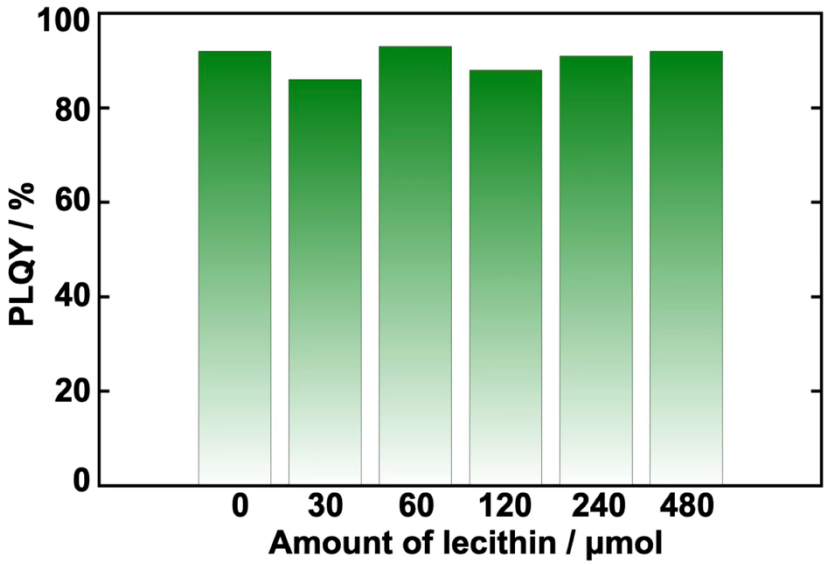

Fig. S7 PLQY variation of PeNCs polymer films with different amounts of lecithin.

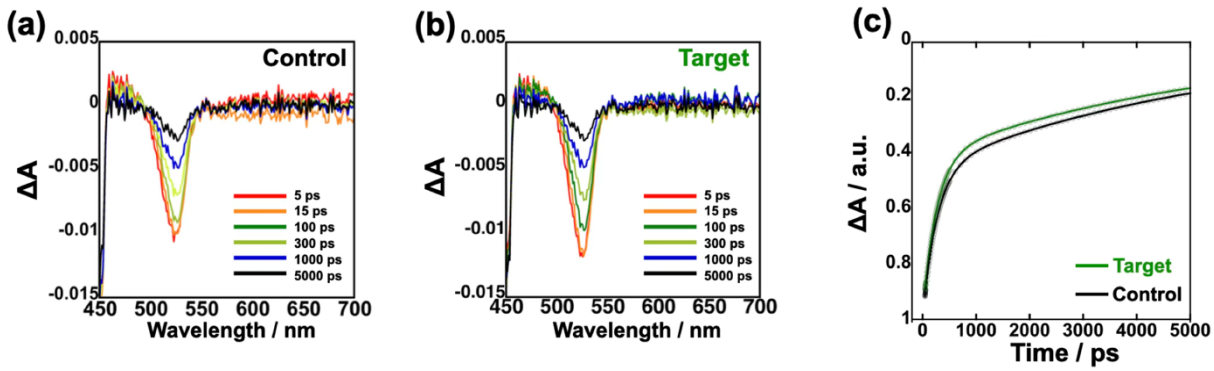

Fig. S8 Transient absorption (TA) spectra of (a) Control and (b) Target samples, at various delay times from 5 to 5000 ps. (c) Normalized TA decay profiles.

Table S7 Fitting parameters of normalized TA decay profiles.

Sample	τ_{avg} / ps	τ_1 / ps	A_1 / -	τ_2 / ps	A_2 / -
Control	2450	261	0.56	5441	0.41
Target	2685	267	0.53	5472	0.46

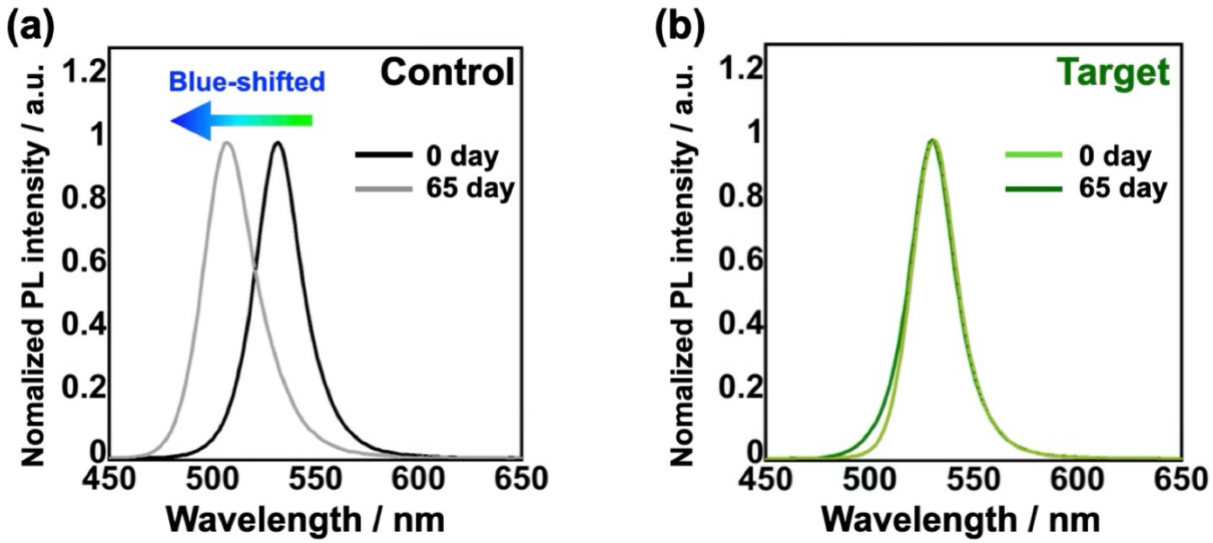

Fig. S9 The results of PL spectra for (a) Control and (b) Target samples in the dispersibility test. The spectra were measured at 0 and 65 days after the washing process using DMC.

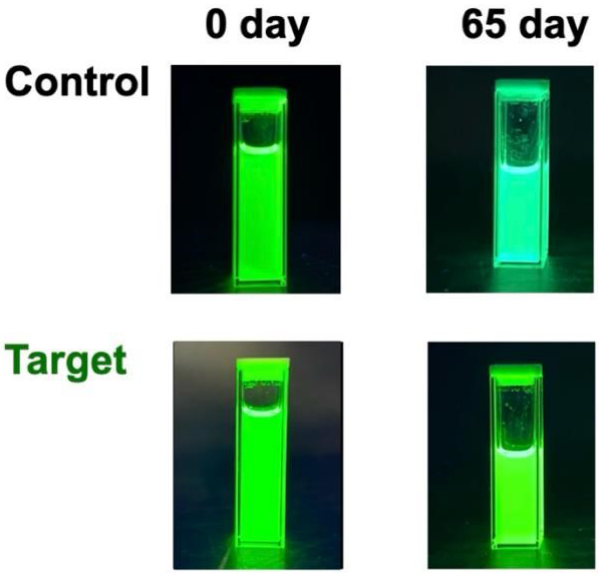

Fig. S10 Photographs of Control and Target dispersions showing dispersibility at 0 and 65 days after the washing process with DMC.

Table S8 The optical properties in PeNC dispersion through the washing process after 65 days

Sample	λ_{PL} / nm	FWHM / nm	PLQY / %
Control	507	31	82
Target	531	25	95

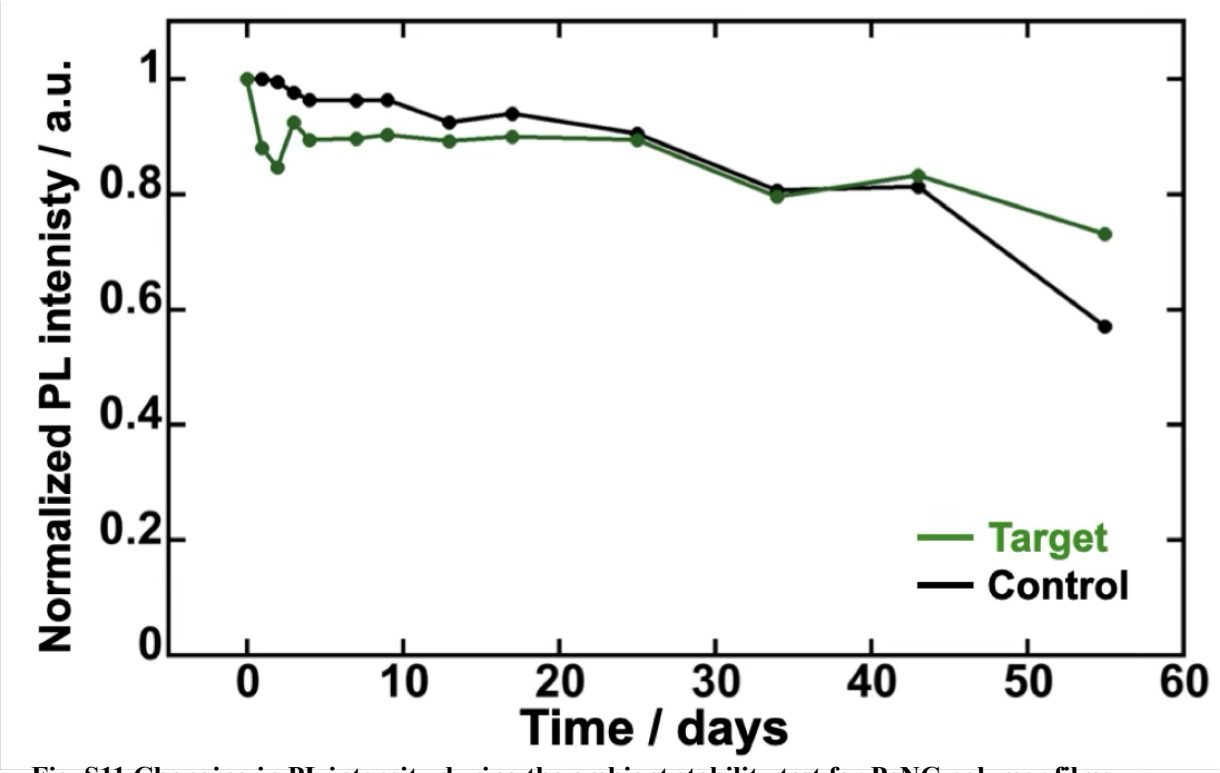

Fig. S11 Changing in PL intensity during the ambient stability test for PeNC polymer films

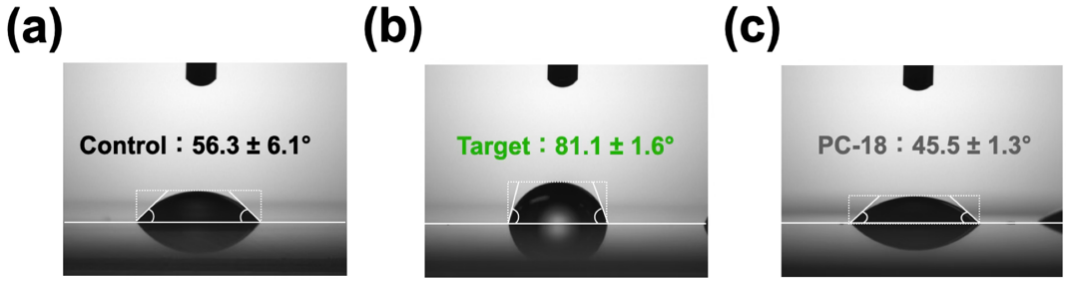

Fig. S12 Contact angle measurements of spin-coated PeNC thin films: (a) Control, (b) Target, and (c) Octadecylphosphocholine (PC-18)—treated samples

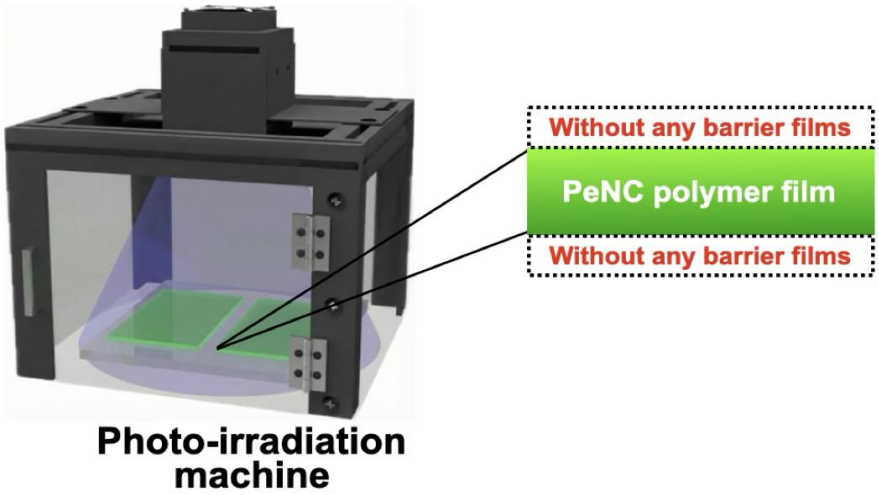

Fig. S13 Schematic illustration of the evaluation setup for photo-irradiation

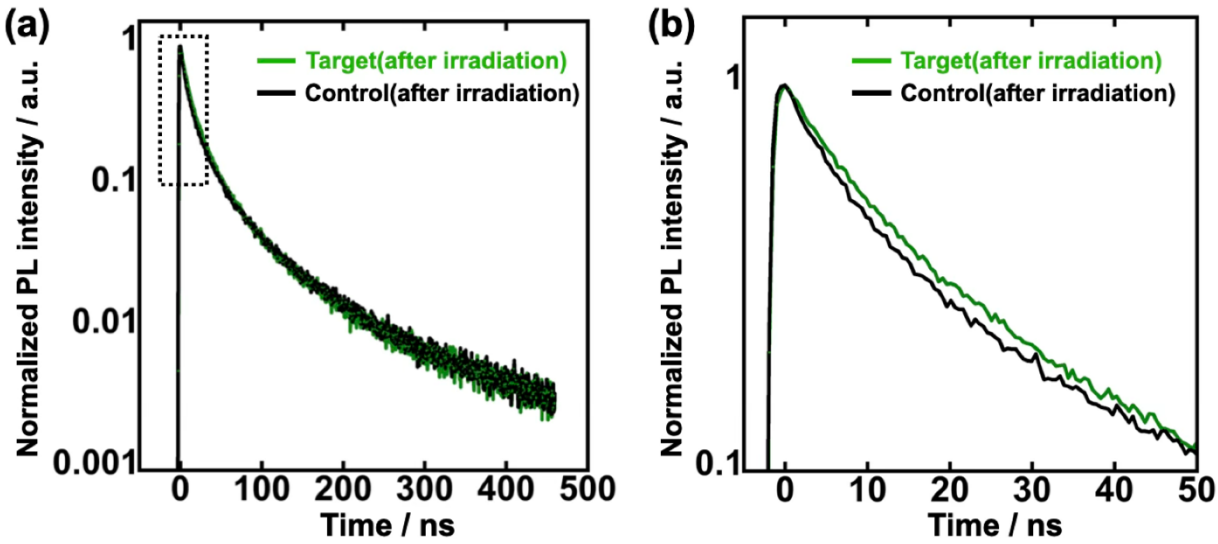

Fig. S14 Time-resolved photoluminescence (TRPL) spectra of the PeNCs polymer films after photo-irradiation. (a) TRPL spectra measured over a 0–500 ns time scale. (b) TRPL spectra in the shorter time scale (0–50 ns), corresponding to the dashed area in (a).

Table S9 TRPL fitting parameters obtained from second-order fitting after 362 h of photo-irradiation

Sample	τ_{avg} / ns	τ_1 / ns	A_1 / -	τ_2 / ns	A_2 / -	K_r / ns^{-1}	K_{nr} / ns^{-1}
Control	15.9	1.1	0.75	18.4	0.25	1.61	4.67
Target	26.1	8.3	0.70	38.4	0.30	2.39	1.44

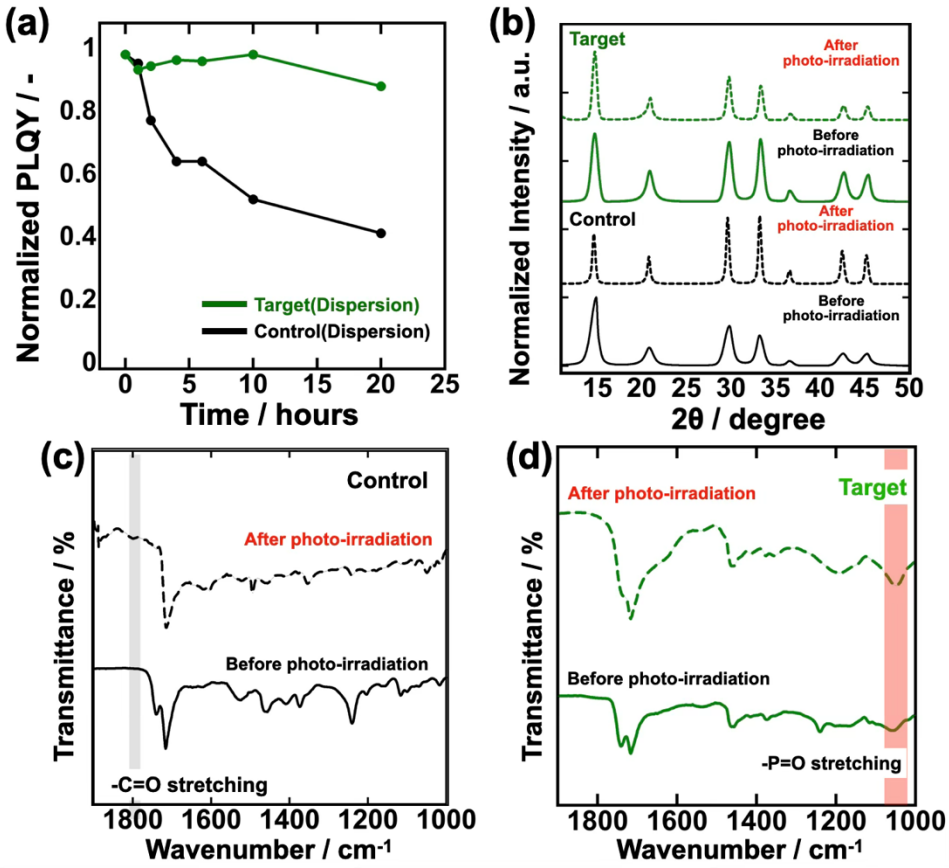

Fig. S15 (a) Photostability test of PeNC colloidal dispersions. (b) XRD patterns of the Control and Target samples before and after photodegradation. FT-IR spectra of the (c) Control and (d) Target samples before and after photodegradation.

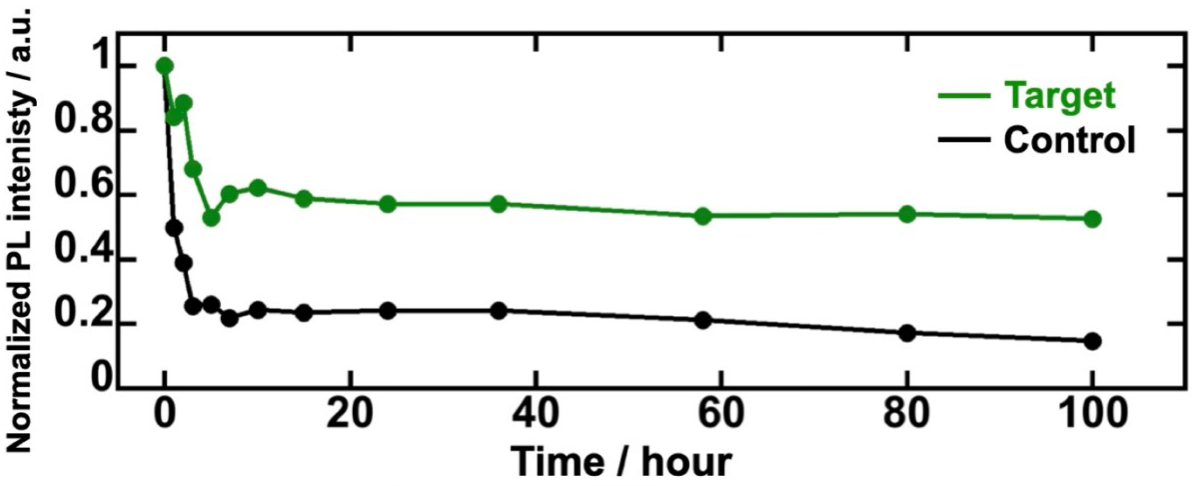

Fig. S16 Photostability of PeNC polymer films under irradiation with accelerated irradiation intensity of 100 mW/cm^2

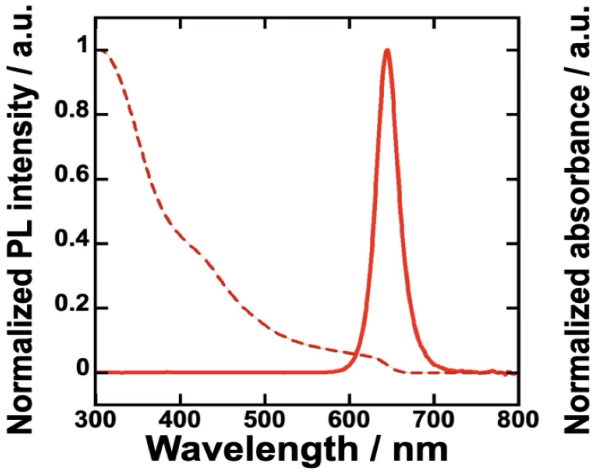

Fig. S17 PL and UV-vis spectra in $CsPbBr_{1-x}I_x$ red-emission PeNCs dispersion

Table S10. Optical properties in $CsPbBr_{1-x}I_x$ red-emission PeNC dispersions

λ_{PL} / nm	FWHM / nm	PLQY / %
649	31	91

Table S11: Summary of previously reported photostability results for the PeNC polymer film.

No.	Composition	Strategies	Form	Irradiation condition	Time	Maintain PL intensity	Reference
1	$CsPbBr_3$	Ligand Eng.	Film	UV	2 h	94%	[3]
2	$FAPbBr_3$	Ligand Eng.	Film	455 nm, 55 mW/cm^2	3 h	70%	[4]
3	$CsPbBr_3$	Ligand Eng.	Film	UV	12 h	73%	[5]
4	$CsPbBr_3$	Ligand Eng.	Film	365 nm, 15 W	45 h	60%	[6]
5	$CsPbBr_3$	Ligand Eng.	Film	365 nm, 22 mW/cm^2	500 h	68%	[7]
6	$FAPbBr_3$	Ion-doped	Film	450 nm, 55 mW/cm^2	12 h	70%	[8]
	$CsPbBr_3$	Silica-courted	Film	365 nm, 80 mW/cm^2	72 h	72%	[9]
7	$FAPbBr_3$	Polymer composite	Film	375 nm, 250 mA	3 h	30%	[10]
8	$CsPbBr_3$	Polymer composite	Film	457 nm, 100 mW/cm^2	10 h	87%	[11]
9	$CsPbBr_3$	Polymer composite	Film	365 nm, 100 mW/cm^2	12 h	60%	[12]
10	$CsPbBr_3$	Polymer composite	Film	455 nm, 0.1 W/cm^2	200 h	52%	[13]
11	**$FAPbBr_3$**	**Ligand Eng.**	**Film**	**450 nm, 30 mW/cm^2**	**354 h**	**50%**	**This work**
12	**$FAPbBr_3$**	**Ligand Eng.**	**Film**	**450 nm, 100 mW/cm^2**	**100 h**	**50%**	**This work**

Table S12: Summary of previously reported water stability results for the PeNC polymer film.

No.	Sample	Strategies	Form	Stability condition	Time	Maintain PL intensity	Reference
1	$CsPbBr_3$	Ligand Eng.	Film	Water immersion	123 h	60%	[6]
2	$CsPbBr_3$	Ligand Eng.	Film	Water immersion	6 days	62%	[14]
3	$MAPbBr_3$	Ligand Eng.	Film	Water immersion	7 days	89%	[3]
4	$CsPbBr_3$	Ligand Eng.	Film	Water immersion	70 days	50%	[15]
5	$CsPbBr_3$	Ion-doped and silica courted	Film	Water immersion	30 days	＞90%	[16]
6	$CsPbBr_3$	Silica courted	Film	Water immersion	50 days	＞95%	[5]
7	$CsPbBr_3$	Polymer composite	Film	Water immersion	240 h	＞95%	[17]
8	$CsPbBr_3$	Polymer composite	Film	Water immersion	10 days	20%	[18]
9	$CsPbBr_3$	Polymer composite	Film	Water immersion	15 days	53%	[19]
10	$CsPbBr_3$	Polymer composite	Film	Water immersion	60 days	＞95%	[20]
11	$CsPbBr_3$	Polymer composite	Film	Water immersion	150 days	<10%	[21]
12	**$FAPbBr_3$**	**Ligand Eng.**	**Film**	**Water immersion**	**42 days**	**93%**	**This work**

3. Reference

1. X. Ren, H.-L. Hu, Z.-Y. Chen, L.-X. Gao, H. Hao, Y. Liu, and F.-L. Jiang, *ACS Applied Nano Materials*, **2023**, *6*, 6092–6102.
2. T. Kimura, K. Yoshida, K. Narazaki, K. Yanagihashi, S. Hirashima, Y. Oyama, K. S. Thakuri, Y. Ito, S. Asakura, M. Kashiwagi, M. S. White, T. Chiba, and A. Masuhara, *Journal of Materials Chemistry C*, **2025**, *13*, 14202–14210.
3. F. Tong, Y. Zhu, Z. Yang, X. Gu, and Z. Chen, *Materials Science in Semiconductor Processing*, **2026**, *205*, 110389.
4. H. Hu, H. Shi, J. Zhang, J. A. Hauch, A. Osvet, and C. J. Brabec, *ACS Applied Nano Materials*, **2024**, *7*, 8823–8829.
5. T. Tian, M. Yang, Y. Fang, S. Zhang, Y. Chen, L. Wang, and W. Q. Wu, *Nature Communications*, **2023**, *14*, 234.
6. R. Meng, Y. Zhou, Y. Wang, M. Li, X. Wang, X. Liu, and J. Lin, *Materials Today Communications*, **2025**, *46*, 112568.
7. Y. Wang, R. Wang, Y. Ge, C. Geng, and S. Xu, *ACS Applied Materials & Interfaces*, **2024**, *16*, 29132–29140.
8. H. Hu, D. Fehn, M. K. S. Barr, C. Harreiss, Y. Zhao, K. Meyer, A. Osvet, and C. J. Brabec, *ACS Applied Materials & Interfaces*, **2024**, *16*, 17946–17953.
9. Y. Hu, S. Kareem, H. Dong, W. Xiong, S. Tian, J. Shamsi, L. Li, X. Zhao, and Y. Xie, *ACS Applied Nano Materials*, **2021**, *4*, 6306–6315.
10. E. Darwish, J. Elia, M. Batentschuk, A. Osvet, and C. J. Brabec, *Advanced Engineering Materials*, **2025**, *27*, 2402713.
11. C. Zhang, Z. He, M. Mogensen, A. J. Gesquiere, C.-H. Chen, T.-L. Chiu, J.-H. Lee, S.T. Wu, and Y. Dong, *Journal of Materials Chemistry C*, **2021**, *9*, 3396–3402.
12. M. Meyns, M. Peralvarez, A. Heuer-Jungemann, W. Hertog, M. Ibanez, R. Nafria, A. Genc, J. Arbiol, M. V. Kovalenko, J. Carreras, A. Cabot, and A. G. Kanaras, *ACS Applied Materials & Interfaces*, **2016**, *8*, 19579–19586.
13. F. Boussoufi, M. Pousthomis, A. Kuntzmann, M. D'Amico, G. Patriarche, and B. Dubertret, *ACS Applied Nano Materials*, **2021**, *4*, 7502–7512.
14. S. Nie, Y. Zhu, X. Bai, X. Gu, X. Wang, L. Zhu, and S. Huang, *Journal of Alloys and Compounds*, **2026**, *1053*, 186208.
15. Y. Lei, L. Bai, H. Liang, J. Cheng, Z. Xu, T. Li, S. Chen, and D. Zhang, *Applied Surface Science*, **2024**, *670*, 160711.
16. F. Ren, F. Chen, E. Mei, X. Liang, P.-C. Qian, and W. Xiang, *ACS Photonics*, **2021**, *8*, 2130–2138.
17. Y. Li, Y. Lv, Z. Guo, L. Dong, J. Zheng, C. Chai, N. Chen, Y. Lu, and C. Chen, *ACS Applied Materials & Interfaces*, **2018**, *10*, 15888–15894.
18. W. Yang, L. Fei, F. Gao, W. Liu, H. Xu, L. Yang, and Y. Liu, *Chemical Engineering Journal*, **2020**, *387*, 124180.
19. Z. Wang, R. Fu, F. Li, H. Xie, P. He, Q. Sha, Z. Tang, N. Wang, and H. Zhong, *Advanced Functional Materials*, **2021**, *31*, 2010009.
20. A. Pan, M. J. Jurow, Y. Wu, M. Jia, F. Zheng, Y. Zhang, L. He, and Y. Liu, *ACS Applied Nano Materials*, **2018**, *2*, 258–266.
21. S. Miralles-Comins, M. Zanatta, A. F. Gualdron-Reyes, J. Rodriguez-Pereira, I. MoraSero, and V. Sans, *Nanoscale*, **2023**, *15*, 4962–4971.